When things add up: environmental structure and microbial interactions drive antibiotic-resistance plasmid evolution

Laurens E. Zandbergen[1], Mishelle Bustamante[1], Jan-Maarten Luursema[2], Thomas Hackl[1], Marjon G.J. de Vos[1*]

1 Groningen Institute of Evolutionary Life Sciences (GELIFES), University of Groningen, Groningen, The Netherlands

2 Radboud University Medical Center, Nijmegen, the Netherlands

*corresponding author: m.g.j.de.vos@rug.nl

Competing interests

The authors declare no conflict of interest.

Abstract

Antimicrobial resistance is recognized as a major global health threat. Pathogens can rapidly evolve resistance which diminishes the impact of antimicrobial treatments. The presence of other microbes in polymicrobial infections can impact the development of antimicrobial resistance of pathogens, yet it is unclear how the interplay between the environmental structure and the presence of a polymicrobial community affect the rate of plasmid mediated antibiotic resistance evolution. This study investigates the effect of environmental structure and microbial interactions on antibiotic resistance evolution in a uropathogenic *Escherichia coli.* We conducted a serial transfer experiment across well-mixed and spatially structured environments with increasing concentrations of trimethoprim-sulfamethoxazole, in the presence and absence of a polymicrobial community. Our results revealed that *E. coli* in community context displayed parallel evolutionary trajectories, leading to higher final antibiotic tolerance, while spatial structures allowed for prolonged resistance evolution. Copy number variation of the plasmid-borne resistance locus varied significantly across the different evolutionary contexts. *E. coli* lineages evolved in the absence of the community, in the well-mixed isolation environments demonstrated the highest copy number increases, while those in the presence of the community showed minimal changes compared to the ancestor. These findings underscore the intricate relationship between the genetic basis of resistance, the environmental structure and the microbial ecology in plasmid-mediated antimicrobial resistance evolution.

Introduction

Polymicrobial communities can have a profound effect on the severity of infections[1–4] and can diminish treatment efficacy of pathogens.[5–8] Pathogens are increasingly becoming resistant to antimicrobials, complicating treatments.[9] According to the World Health Organization, antimicrobial resistance (AMR) is among the top ten of threats to global health.[10]

Emerging research shows that AMR can be a collective trait that develops within bacterial communities.[7,10,11] For example, tolerance to antibiotics can be increased in a community by decreasing antibiotic pressures in the local environment through antibiotic degradation, leading to increased pathogen density.[12–14] Higher population densities have been shown to reduce the susceptibility to certain antibiotics, which is known as the inoculum effect.[15,16] However, microbial communities are more often driven by competition rather than cooperation, which would lead to a reduction in average population size per member and therefore a change in survival.[17] Yet, cooperation occurs and it has been observed that interspecies interactions can lead to antibiotic protective effects.[10,18]

The environmental structure of bacterial communities can have a large impact on bacterial growth. Virtually all known bacteria are capable of creating biofilms or attach to surfaces, which enhances tolerance to environmental stressors, both biotic and abiotic.[19,20] Spatial growth versus growth in a well-mixed environment has different effects on the selective pressures and growth of bacterial populations, such as alterations in competitive and mutualism dynamics.[21,22] Environmental structure has been implicated as a critical factor for the stability and coexistence of species in a community.[23–25] For example, gene expression related to quorum sensing, and consequently antibiotic susceptibility,[26] is different in a spatially structured system compared to a well-mixed environment.[27] Importantly, theorical and empirical research suggests that social interactions of bacteria in spatially structured environments are significantly altered compared to environments with better mixing, leading to different survival outcomes.[28–31]

Different environmental structures can alter the ecological interactions of microbes. Such different ecological interactions can subsequently affect microbial co-existence and evolution.[23–25] Here we seek to investigate the effect of the environmental structure on antibiotic resistance evolution of a focal pathogenic species in the presence and absence of a four-member microbial community, and in two contrasting environments, a well-mixed liquid and a spatially structured solid environment. Previous studies indicated that populations in spatially structured environments adapt more slowly than those in well-mixed environments and evolution in a spatially structured environments increases genetic drift and founder effects on local populations reducing the rate of adaptation.[21,32] It has also been shown that spatial

structures promote species coexistence and that there is a decrease in metabolite exchange in continuously mixed environments.[33,34] Based on these studies, we hypothesized that the evolution of resistance will be slower in a spatial environment,[21,32,35,36] and that in the well-mixed environment the focal species will be less able to benefit from the presence of the community members.[33,34]

Results

Environmental structure and microbial community impact evolutionary trajectories

To study the effects of structure and community context on the evolution of antibiotic resistance, we evolved a uropathogenic isolate of *E. coli* carrying a plasmid encoding resistance genes that only confer low resistance in a serial transfer evolution experiment. Evolving cultures were transferred bi-daily over 120 days, in artificial urine medium (AUM) containing increasing levels of trimethoprim-sulfamethoxazole, under four different conditions. Specifically, five replicates of *E. coli* per condition were evolved in both a well-mixed and spatially structured AUM environment, both in the presence and absence of a community of three other bacterial species. These other species are often co-isolated with *E. coli*; *Klebsiella pneumoniae, Enterococcus faecium* and *Staphylococcus epidermidis* in polymicrobial urinary tract infections (Materials and Methods).[37] During the serial transfer experiment antibiotic concentrations were increased by 20%, depending on whether the population size of the *E. coli* focal species exceeded a certain threshold. Thresholds were set at colony size exceeding >1 mm (which is an increase of 20% colony size at minimum) for the spatially structured environments. And at $>1*10^6$ colony forming units (CFU)/mL for the liquid environments. Because colonies could only be counted the day after a transfer, the population size at the previous transfer was taken as the threshold. Therefore, the fastest rate of antibiotic increase was every other transfer. Community members, other than *E. coli*, already had high resistances to trimethoprim and sulfamethoxazole (>1 mg/mL), and were always present at a low density in the community at the start of each transfer ($<10^5$). To prevent their loss during the serial transfer experiment, a 100x dilution of wild-type stationary phase monocultures of the community members was added at each transfer together with a 100x dilution of the *E. coli* from the previous step (Materials and Methods). The initial concentration of antibiotics was 50% of the *E. coli* minimum inhibitory concentration (MIC) for the 1:5 ratio of trimethoprim-sulfamethoxazole, 42 µg/mL trimethoprim (TMP) and 210 µg/mL sulfamethoxazole (SMX). This ratio was picked to resemble the ratio used in clinical settings.[38]

105 Observing the level of antibiotic increase of *E. coli* per replicate lineage in each condition, we
106 find that the five replicate phenotypic evolutionary trajectories overlapped in three of the four
107 conditions. Particularly, the replicate lineages overlapped for *E. coli* evolved in the spatially-
108 structured environments in the presence and absence of the community, and *E. coli* evolved
109 in the well-mixed environment in the presence of the community (Figure 1AB). The presence
110 of the community seemingly leads to the canalization of the phenotypic evolutionary
111 trajectories of *E. coli* in the well-mixed environment. In contrast, *E. coli* evolved in isolation in
112 this same well-mixed environment had markedly increased divergent phenotypic evolutionary
113 trajectories. We observed a 3.5x difference in antibiotic concentration between the replicates
114 with the highest (1.92:9.58 mg/mL TMP:SMX) and lowest (0.54:2.68 mg/mL TMP:SMX)
115 antibiotic concentration at the final transfer (Figure 1A). Evolution in the spatially structured
116 environments did not lead to a difference in the divergence of phenotypic evolutionary
117 trajectories, as all five replicate trajectories overlapped (Figure 1B).
118
119 For the three overlapping replicate trajectories, the rate of evolution in the first few weeks were
120 close to the hypothetical maximum rate. For the well-mixed environment, this is until day 80,
121 and the spatially structured environment until day 48 for the *E. coli* evolved in presence of the
122 community and day 30 for *E. coli* evolved in isolation. (Figure 1AB). This suggests that within
123 these environments, selective pressures drove evolution in a specific direction, potentially
124 funneling evolution towards similar evolutionary outcomes creating the strong convergence of
125 the trajectories.
126
127 The final concentration of antibiotics that the evolved *E. coli* populations can sustain is higher
128 in the community context compared to in isolation (2.3:11.5 mg/mL vs. 1.9:9.5 mg/mL
129 TMP:SMX in the well-mixed environment and 4.0:20 mg/mL vs. 2.8:14 mg/mL TMP:SMX for
130 the spatially-structured environment). This shows that the presence of the community had a
131 positive impact on the level of antibiotics that *E. coli* could sustain in both the well-mixed as
132 well as the spatially structured environment (P=0.023 for the community impact in the well-
133 mixed environment and P<0.001 for the community impact in the spatially structured
134 environment, *Welch's t-test*).

135 Additionally, the structure of the environment, either the well-mixed AUM or spatially structured
136 AUM-agar, had an impact on the evolutionary trajectories of *E. coli*. Initially, for both well-
137 mixed and spatially structured environments, the rate of antibiotic increase was identical.
138 However, after the first 50 days of evolution (25 transfers) the trajectories started to diverge.
139 The rate at which the antibiotic could be increased dropped slightly for the spatially structured
140 community environment, compared to the well-mixed community environment. Despite the

141 fact that the spatially structured environment enabled a slower rate of antibiotic increase, the
142 concentration of antibiotics at the final transfer of the evolution experiment is higher in the
143 spatially structured environments, compared to the well-mixed environment (Figure 1B). The
144 antibiotic increase in the well-mixed environment stagnated around day 108. Yet the rate of
145 evolution in the spatially structured environment had not stagnated (>10 days without antibiotic
146 concentration increase) at the final transfer. We cannot exclude that the solvents used for the
147 antibiotic stocks could also impact the fitness of the *E. coli* and community members,
148 particularly at the end of the experiments when antibiotic concentrations are high. The final
149 concentration of TMP:SMX in the spatially structured environments the concentration was
150 4:20 mg/mL for the *E. coli* in the presence of the community and 2.8:14 mg/mL for the isolated
151 *E. coli*. The concentrations in the well-mixed environment were lower; in the presence of the
152 community, 2.3:11.5 mg/mL, and the highest level of the isolated *E. coli,* 1.9:9.5 mg/mL. Yet,
153 these results indicate that the environmental structure, well-mixed in AUM or spatially
154 structured on AUM-agar, differentiated the course of the evolutionary trajectories (one-way
155 ANOVA, $P<0.001$ for liquid vs. solid).

156 These results show that both the presence of the community, as well as the structured
157 environment had an impact on the evolutionary trajectories of trimethoprim-sulfamethoxazole
158 resistance of *E. coli*. Notably, community context led to an increased parallelism of
159 evolutionary paths and higher final antibiotic tolerance, while spatial structure allowed for
160 longer sustained resistance evolution and higher final antibiotic concentrations compared to
161 the well-mixed environments.

162

163 **Community interactions mediate response to selection**

164 Uropathogenic *E. coli* is known for its flexible metabolism, being able to adapt and respond to
165 fluctuating nutrients in the environment.[39] We questioned whether *E. coli* would respond
166 differently to the presence of antibiotics in the presence of the community. We observed that
167 the focal *E. coli* population is a good competitor in the AUM environment, both in the well-
168 mixed and spatially structured environments. It is also able to outgrow the other community
169 members. For example, in the first 30 days the density of *E. coli* was between the 10^8 and 10^9
170 CFU/mL for most replicates at the time of transfer in the well-mixed environment in the
171 presence of the community. Such a high population density was maintained even when
172 antibiotic reached the initial MIC after 12 days. Even though the community members are
173 highly resistant (>1:5 mg/mL TMP:SMX), *E. coli* is able to reach higher abundances from the
174 onset of the experiment. In the absence of the community, we observe lower abundances of
175 *E. coli* in the well-mixed environment at the time of transfer (Figure 1C) ($P<0.001$ for the first

176 30 days, ANOVA). Also on the spatially structured environment, colonies of *E. coli* surrounded
177 by the community members were much larger in surface area (~3x) compared to *E. coli*
178 colonies surrounded by other *E. coli* colonies (Figure 1D) (P<0.001 for the difference between
179 community and isolation colonies, *Welch's t-test*, *Materials and Methods*). The population
180 sizes of the five replicates lineages evolved within the same environment were similar (Figure
181 1CD, P>0.05, independent samples t-test with Bonferroni correction).

182 The presence of the three-species community benefits the *E. coli* antibiotic resistance
183 evolution rate. In the presence of the community, it takes 12 days before *E. coli* lineages pass
184 the wild type MIC level. In isolation that takes longer, after 16-18 days (P<0.001, ANOVA).
185 Despite larger colony sizes in the presence of the community, all replicates, in the presence
186 of the community as well as in in isolation, reached the native MIC after 12 days in the spatially
187 structured environment.

188 The beneficial effects of the community weaned off over time. For the well-mixed environment,
189 after around 80 days the rate of antibiotic increase slowed down (Figure 1A, dark blue graph).
190 Interestingly, this occurred for all five replicates at the same time, which suggests that the
191 community canalizes the phenotypic trajectories in a general manner. We do not observe such
192 a synchronization of the phenotypic evolutionary trajectories for the replicate lineages of *E.*
193 *co*li in isolation (Figure 1A, light blue graphs). In the spatially structured environment, we also
194 find such a synchronized slow-down, yet at another time point (48 days) and antibiotic
195 concentration (446:2229 µg/mL in solid vs. 1917:9585 µg/mL in liquid TMP:SMX). In this
196 spatially structured environment, the canalization of the phenotypic trajectories is not confined
197 to the replicates evolving in the presence of the community only. We also observe the
198 canalized phenotypic trajectories for the isolated *E. coli*. Yet, similarly to the growth in the well-
199 mixed environment, the slow-down of the rate of antibiotic increase occurs earlier for *E. coli*
200 evolved in isolation. *E. coli* in isolation started diverging from the *E. coli* in the presence of the
201 community after 28 days (179:896 µg/mL TMP:SMX).

202 The population sizes of the community members also decreased over time. *K. pneumoniae*
203 was present abundantly in the well-mixed environment at the start of the experiment (between
204 10^7 and 10^8 CFU/mL), this decreased steadily to between 10^6 and 10^7 CFU/mL after 14 days.
205 *K. pneumoniae* was not detected later in the experiments, meaning it had an abundance of at
206 least 100-fold lower than *E. coli*, which would be under the detection limit. Also in the spatially
207 structured environment, *K. pneumoniae*¸ measured by its colony size, steadily decreased in
208 size during the first 14 days, in accordance with the *K. pneumoniae* population size in well-
209 mixed environment. The colonies of *K. pneumoniae* kept decreasing with every increase in
210 antibiotics, showing that increasing antibiotic concentrations affects the wild-type *K.*

211 *pneumoniae* fitness negatively (average colony size at day 2 14494 pixels, at day 120 8518
212 pixels). *E. faecium* was always present in low numbers, around 10^2 -10^3 CFU/mL, as expected
213 from previous studies,[4,10] yet population sizes became smaller with increasing antibiotic
214 concentrations decreasing at least 5x between the start and the end of the 120 days.
215 Surprisingly, *S. epidermidis* was hardly detected during the experiments, indicating population
216 sizes below 10^3 CFU/mL, even though *S. epidermidis* cultured in isolation is more abundant
217 than *E. faecium* (10^4-10^5 CFU/mL). It is likely that competition with other species, or the
218 increasing antibiotics concentrations hindered *S. epidermidis* to thrive, even though it can
219 survive high concentrations[8]. The decrease of both the focal species and community members
220 over time could point to an increase in competition, a decrease in cooperation or a fitness
221 decrease due to the increase in antibiotics concentration in the environment.

222

223 **Environmental structure and community effect on antibiotic resistance**

224 Next, we investigated how the two differently structured environments (spatially structured or
225 well-mixed) had affected the evolutionary outcome of antibiotic resistance evolution.
226 Comparing the *E. coli* lineages that evolved in isolation with the lineages that evolved in the
227 presence of the community, we find that the well-mixed environment and the spatially
228 structured environment had a different effect on the final level of antibiotics. Despite that the
229 lineages evolved in the spatially structured environment tolerated higher concentrations of
230 antibiotics at the end of the experiment compared to the well-mixed environments (Figure
231 1AB), we find that replicates evolved in the spatially structured environment had a lower MIC
232 than those in the well-mixed environment in the presence of the community (resp. 0.8:4 mg/mL
233 TMP:SMX and 3.2:16 mg/mL TMP:SMX, Figure 2A, Materials and Methods). It is possible that
234 the surface growth mode or spatial adaptation during the evolution experiments impacted the
235 fitness and antibiotic susceptibility measurements in liquid.

236 A similar observation can be made for *E. coli* evolved in isolation in both environments. In the
237 spatially structured environment, the concentration of antibiotics that could be tolerated at the
238 final transfer is higher than that in the well-mixed environment. Yet, the MIC of *E. coli* evolved
239 in the spatial environment was generally lower (MIC 0.92:4.6 mg/mL TMP:SMX spatially
240 structured environment, versus MIC of 1.06:5.3 mg/mL TMP:SMX for three of the five
241 replicates from the well-mixed environment (P<0.001, *Welch's t-test*). The other two replicates
242 in the well-mixed environment had a lower MIC (0.27:1.33 and 0.13:0.66 mg/ml TMP:SMX
243 respectively), and corresponded to those lineages that could sustain a lower final
244 concentration of antibiotics in the evolution experiment (Figure 1A, light blue graphs, Figure
245 2A)).

Based on the observation that the population size increased in the presence of community members, we hypothesized that *E. coli* had benefited from the presence of one or more of the community members during the evolution experiment. To investigate the effect of the community on the evolved resistance of all evolved lineages, we measured the minimum bactericidal concentration (MBC) of antibiotics at which we could not observe our focal species anymore when cultured in the presence of the community (Figure 2B, Figure S1 , Materials and Methods). We find that replicates evolved in the well-mixed environment in absence of the community could sustain twice the concentration of antibiotics when cultured in the presence of the community (MBC of 1.6:8 mg/mL TMP:SMX for 3 out of 5 replicates), compared to their MIC without the community of 0.8:4 mg/mL TMP:SMX for those same replicates) (Figure S1). Yet, for the replicates evolved in the well-mixed environment in presence of the community, we observed a decrease in MBC compared to the MIC in presence of the community (MIC of 3.2:16 mg/mL TMP:SMX, MBC 1.6:8 mg/mL TMP:SMX). This means that the community negatively affected the growth of *E. coli* lineages that were evolved together with the community members in the well-mixed environment. Interestingly, *E. coli* replicates evolved in the spatially structured environment benefited from the presence of the community members; these could sustain a two-fold increase in the level of antibiotics compared to the MIC (Figure 2B). These results show that generally, the community has a positive effect on antibiotic tolerance of *E. coli*, even after resistance evolution, except when *E. coli* was evolved in the presence of the community in the well-mixed environment.

We find that the positive effect of the community eventually decreases over time, with increasing antibiotic concentrations (Figure 1CD). An explanation might be the adaptation to the environment itself. As the medium used is relatively poor, it is possible that adaptation to it leads to niche overlap of the focal species with other microbes in the community and therefore more competition,[40] which would correspond with theory suggesting stronger selection in well-mixed environments.[41,42] Alternatively, when antibiotic resistance in *E. coli* increases, the protective effect of the community becomes less beneficial, and *E. coli* may switch to a more competitive state to benefit from the limited resources. Particularly from the spatially structured perspective, theory suggests that communities benefit more from public goods interactions than they would in well-mixed environments,[30,31,43] which could potentially explain why the *E. coli* replicates evolved in the spatially structured community environment could still benefit from the presence of the community compared to those evolved in the well-mixed environment, as public goods interactions might still be prioritized over competition.

281 **Copy number variation of resistance loci on plasmid**

282 To generate insights in the genetic basis underpinning the evolved resistance, we sequenced
283 three clones of the final transfer of each of the five replicate lineages evolved in each condition,
284 and compared these sequences to that of the ancestor (Materials and Methods). A likely target
285 for evolutionary selection is the *folA* (dihydrofolate reductase) gene, which is known to
286 increase resistance against trimethoprim.[44] We found no evidence however for mutations
287 within the *folA* gene in any of the evolved lineages. We did observe an identical frameshift
288 mutation in the *folP* gene in two of the five *E. coli* replicates evolved in the well-mixed
289 environment in the presence of the community (Table S1). The product of which
290 (dihydropteroate synthase) is inhibited by sulfamethoxazole.[38] Disruption of this gene leads to
291 increased sulfamethoxazole tolerance as it leaves more resources for the remaining proteins
292 of the folate pathway and removes a target for the antibiotic itself.[45] However, this mutation, in
293 conjunction with the other mutations in these replicates, does not yield significant population
294 size differences compared with the other three replicates evolved within the same environment
295 (P>0.05, independent samples t-test with Bonferroni correction).

296 We did not find any other chromosomal mutations in genes known to confer resistance in the
297 evolved populations (Table S1). The ancestral strain, despite being highly sensitive to the start
298 concentration of TMP-SMX at the beginning of the experiment, did however contain a 138K
299 base pair sized IncFII-plasmid that contains genes annotated to encode for resistance against
300 both antibiotics, *dfrA17* and *sul1,* respectively. *DfrA17* confers resistance to trimethoprim, s*ul1*
301 encodes a dihydropteroate synthase, conferring resistance to sulfamethoxazole. These
302 resistance genes are located in an Tn21-like integron cassette, which is similar to a cassette
303 first described by Liebert in 1999 (Figure S2).[46] Although at that time, the transposon did not
304 contain the *dfrA17* gene, or any of the other resistance genes located on that cassette, yet.
305

306 The lack of genetic substitutions in the antibiotic resistance targets on the chromosome,
307 pointed in the direction of resistance associated with the plasmid-encoded resistance genes.
308 Therefore, we assessed the copy numbers of the plasmid in the evolved clones and in the
309 ancestor. The *E. coli* ancestor contained two copies of the plasmid relative to the host
310 chromosome (Figure 3A). The replicate clones of the final transfers had a similar number of
311 copies, this could therefore not explain the increased resistance level. However, there were
312 variations in the integron cassette containing the antibiotic resistance genes. The copy number
313 variations (CNVs) of this cassette do not correlate with the MIC (R^2=0.12, P=0.13, Figure 3B).
314 Surprisingly, some of the lineages evolved in isolation in the well-mixed environment had a
315 relatively low MIC although these contain higher copy numbers of the antibiotic-resistance
316 genes (Figure 3B). This suggests that either the increased copy number of transposable

317 elements has a negative effect on the fitness of *E. coli*, or the MIC is not only determined by
318 the copy number variation of the resistance genes, but also by the environment, other
319 mutations or the location of integration. Naturally, all these parameters could simultaneously
320 affect the level of resistance[47], and we did previously observe that the environment affects the
321 fitness of our focal species.[4,10]

322 Zooming in on the resistance locus where the *dfrA17* and *sul1* genes are located, we found
323 substantial copy number variation across conditions, replicates and even clones from the
324 same replicate and environment. Resistance locus abundance ranged from 0 copies, meaning
325 a complete deletion, in one well-mixed environment clone evolved in the presence of the
326 community, to 14 copies relative to the host chromosome for one clone evolved in the well-
327 mixed environment in the absence of the community(Figure 3A, Figure S3). Overall, resistance
328 locus copy numbers were highest in clones that were evolved in isolation, in the absence of
329 the community, in the well-mixed environment (median 5.2) and in the spatially structured
330 environment (median 3.4). Copy numbers in *E. coli* evolved in community context were
331 seemingly unaffected across the majority of clones (median 1.7 in the well-mixed and 2.0 in
332 the spatially structured environment). Across all conditions, some replicate lineages or
333 individual clones deviated from the overall trend. For example, in the well-mixed community
334 context most clones showed no deviations from ancestral copy-numbers, yet replicate 3
335 clones showed copy number increases and two replicate 4 clones showed decreases to 1 and
336 0 copies respectively (Figure S3). Compared to the isolates evolved in the well-mixed
337 environment in isolation, each evolutionary context showed significant difference in resistance
338 locus CNV (well-mixed community (P=0.0030), spatially structured isolation (P=0.025) and
339 spatially structured community (P=0.024), *Welch's t-tests*). There was also a significant
340 difference between the *E. coli* clones evolved in the well-mixed community environment and
341 the spatially structured isolated environment (P=0.018). Yet, there were not significant
342 differences between the spatially structured environments (P=0.87) and the two environments
343 with the community present (P=0.059). This shows that the presence of the community and
344 the environmental structure during evolution mediate the antibiotic resistance loci copy
345 number variation.
346
347 The implications of these data are multifaceted: overall, we found that lineages evolving
348 antibiotic resistance in isolation had higher copy numbers of the *dfrA17-sul1* resistance locus,
349 suggesting selection for higher copy numbers of these genes in resistance evolution under
350 these conditions. Lineages evolving in the community context, however, showed no CNV
351 increase in the majority of replicates and clones (7 out of 10 replicates or 20 out of 30 clones),
352 and moderate copy number increases in three replicates, suggesting a different selective

353 context. We had previously noticed that the community positively affects the growth of *E. coli*.
354 We hypothesize that this physiologically conferred tolerance explains the higher tolerance to
355 the antibiotics and, in turn, reduced selection for increased copy numbers of resistance genes
356 for *E. coli* cultured in the presence of the community.

357 The high level of CNV variation of the integron cassette containing the antibiotic resistance
358 genes both across and within replicates, suggests high heterogeneity within replicate
359 populations and points towards a dynamic process with high copy numbers as a potentially
360 unstable state, possibly maintained by high selective pressure. This hypothesis is in line with
361 an insertion-sequence-driven copy mechanism for the resistance locus that can quickly
362 generate new copies in a stochastic manner under stress but, at the same time, increases
363 genomic instability by multiplying the chances for disruptive random insertions or deleterious
364 homologous recombination with every new copy. Such negative feedback could facilitate the
365 simultaneous generation and continuous purging of excess resistance locus copies in plasmid
366 lineages and explain the high level of inter-clonal variation we observe.[48]

367

368 **Environmental and community context modulate genetic adaptation**

369 The number of mutations within the genome of *E. coli* mutants differed significantly between
370 environments. In the well-mixed environment, we observed 25 mutations in total for all clones
371 of *E. coli* evolved in isolation and only 16 mutations in clones evolved in the presence of the
372 community. For the spatially structured environment we observed 45 mutations for those
373 evolved in isolation and 48 for those evolved in the community context (P=0.004, *Welch's t-*
374 test for the difference between the well-mixed and the spatially structured environments). This
375 fits our expectations, as the spatially structured environment interactions are limited to the
376 cells in close proximity, leading to increased genetic drift within the population,[49] and a lower
377 chance of beneficial mutations sweeping through the population. The mutations observed,
378 with the exception of *folP*, are, as far as we are aware of, not directly linked to antibiotic
379 resistance to TMP-SMX.[50–52]

380 Due to the parallel evolutionary trajectories of many of our replicates evolved in the same
381 environment (Figure 1AB), we hypothesized to see similar genetic substitutions of lineages
382 evolved under similar circumstances. As a measure of genetic parallelism, which takes into
383 account the fraction of shared mutations between two isolates we calculated the *H-index*,[50]
384 (Materials and Methods) on both the gene-level and the Cluster of Orthologous Group (COG)
385 level (Figure 4) for substitutions in the *E. coli* chromosome. In the H-index, a value of 0
386 indicates no shared mutations and a value of 1 indicates that all mutations are shared between
387 the two mutants. Previously, we have seen quite a high degree of genetic parallelism in

388 replicate populations evolved under the influence of TMP-SMX in the presence of other
389 bacterial isolates.[14] Here, besides the CNV of the resistance genes on the Tn21-like integron
390 cassette, we hardly find any such genetic parallelism, except between replicates evolved in
391 the same spatially structured environment (Figure 4A). This indicates that, for the well-mixed
392 environment, unique mutations were found in each of the replicates (Table S1). An exception
393 are two *E. coli* replicates that were evolved in the well-mixed environment in the presence of
394 the community, that had only one gene which was repeatedly mutated within the genome.
395 This mutated gene, *folP*, which as mentioned before is targeted by sulfamethoxazole, would
396 allow *E. coli* to survive higher antibiotic pressures.[51]

397 In replicate lineages that had evolved on the spatially structured environment in the presence
398 of the community, two distinct sets of genotypes evolved. Two replicate lineages had an *H-*
399 *index* value of 0.75, but shared no mutations with the other three replicate lineages evolved
400 under the same environmental circumstance. These two replicates shared mutations in the
401 *treC* gene. This gene is involved in the trehalose degradation pathway, creating glucose and
402 glucose-6-phophate from trehalose-6-phosphate and the mutation of this gene points to
403 adaptation to the nutrients in the environment rather than the antibiotics.[52] The other three
404 replicates evolved in the spatially structured environment with the community also had an *H-*
405 *index* of 0.75 for each pairwise comparison, but also did not share any mutations with the other
406 two replicate lineages. These three replicate lineages incorporated mutations in the *pfkA, traC*
407 and *mpl* genes. One of these genes, *traC* is involved in the type IV secretion system, which
408 plays a role during conjugation.[53] The *traC* gene specifically is involved during cell-cell contact
409 within conjugation, being a component of the pili used within the secretion system.[54] Other
410 studies suggest that *traC* also plays a role in pheromone signaling, being a pheromone binding
411 extracellular protein.[55,56] The mutation in both replicates is a synonymous mutation, potentially
412 not affecting fitness or function, except perhaps through codon bias.[57] The other genes, *pfkA*
413 and *mpl* play a role in carbohydrate degradation and cell wall biogenesis respectively. The
414 *mpL* gene contains a frameshift mutation, leading to a loss of function. The gene encodes
415 UDP-N-acetylmuramate, part of the cell-wall recycling machinery.[58] The *pfkA* gene contains
416 either missense mutations or an in-frame deletion. The gene encodes phosphofructokinase,
417 and is part of the glycolysis pathway. *PfkA* is responsible for about 95% of
418 phosphofructokinase activity in *E. coli.*[59] Deletion of *pfkA* leads to a break in the glycolysis
419 pathway, shifting fructose 6-phosphate availability to other pathways such as the pentose
420 phosphate pathway, which is important for the generation of NADPH.[60]

421 One gene that had a mutation in all replicates for the *E. coli* evolved within the spatially
422 structured environment in isolation was the *nadR* gene, which is part of the NAD salvage
423 pathway.[61,62] This gene converts β-nicotinamide D-ribonucleotide into diphosphate and NAD^+.

424 The involved mutations are either missense mutations or deletions, leading to an inactive
425 variant. Inhibition of this gene has been shown to increase cellular NAD/NADH. NADH itself
426 is an important regulator for enzymes involved in metabolism, it is therefore possible that the
427 mutations within *nadR* are an adaptation to the nutrients in the environment rather than the
428 antibiotics.[63] However, higher levels of cellular NADH have also been linked to contribute to
429 efflux-mediated antibiotic resistance.[63] Four out of five of the replicates also had mutations
430 within the *adhE* gene, which encodes aldehyde-alcohol dehydrogenase.[64] It catalyzes the
431 reaction of acetaldehyde into acetyl-CoA, also creating NADH in the process.

432 Overall, evolution within the spatially structured environments containing TMP-SMX led to
433 mutations within genes leading to increased cellular NADH/NADPH within *E. coli* for eight out
434 of ten replicates. A previous study described to importance of NADPH for the stabilization of
435 the dihydrofolate reductase-ligand complex,[65] with changes in this complex being signs of
436 trimethoprim resistance. Interestingly, the eight replicates with mutations that potentially lead
437 to increases in cellular NADH/NADPH are also the replicates with increased copy numbers of
438 *dfrA17* (Figure 3A), suggesting that the mutations in *nadR, adhE* and *pfkA* are co-adaptations
439 correlated with increases in resistance gene copy numbers of replicates evolved in the
440 spatially structured environment.

441 Additionally, mutations within prophages were observed in the mutant *E. coli* chromosomes
442 (Table S1). Especially in the spatially structured environments SNPs and complex insertions
443 occurred. These mutations were excluded in the primary analysis of mutational patterns in this
444 study, as phage activity was not followed during the evolutionary experiment.

445 We observed more evolutionary parallelism at the COG-level, in accordance with previous
446 research (Figure 4B).[50,66] Again, most similarities are found within the replicates evolved in the
447 spatially structured environments. For these groups of replicates, either in the presence or
448 absence of the community, it can be observed that evolution within these environments lead
449 to both parallel genotypic (Figure 4) and parallel phenotypic (Figure 1AB) adaptation. In
450 contrast, we do not find genomic parallelism corresponding to the parallel phenotypic
451 adaptation of lineages evolved within the well-mixed environment, in the presence of the
452 community. This defeats our expectation that there would be more parallelism in these
453 lineages evolved in the well-mixed environments, due to stronger selective forces and larger
454 population sizes. Furthermore we find that genetic adaptations, at different levels of
455 organization, such as on the integron cassette harboring resistance genes, and the genomic
456 background, potentially to accommodate the CNV changes in the integron resistance
457 cassette,have played a role in the adaptive process. Yet, the observed canalization of
458 antibiotic resistance phenotypes could not entirely be explained by the genetic substitutions

459 only, indicating the importance of another level of interaction, namely the microbial community.
460 This shows multiple levels of genetic and ecological organization dictate antibiotic resistance
461 evolution.

462

463 **Discussion**

464 We observed that the presence of a community has a protective effect on *E. coli* at the start
465 of the antibiotic resistance evolution experiment. This effect decreases with increasing
466 antibiotic concentrations. The presence of the community leads to a faster evolutionary
467 response in both the well-mixed liquid as well as spatially structured solid environments. This
468 corresponds to previous findings in which the presence of other bacteria can speed up and
469 canalize evolution.[14] We observed phenotypic parallelism in each environmental context,
470 either community or environmental structure. For the spatially structured environment, the
471 phenotypic parallelism is linked with genotypic parallelism at the genome level. Yet, for the
472 well-mixed environment, the phenotypic canalization in the presence of the community cannot
473 solely be explained by genomic changes, showing that phenotypic plasticity likely played an
474 important role in the evolutionary response to antibiotics.

475 The beneficial effect of the community on *E. coli* at sub-MIC levels has been observed
476 before.[8,67] Yet, we also observed that the beneficial effect on the fitness of *E. coli* continued
477 even after antibiotic concentrations reached levels above initial MIC. The AUM environments
478 are relatively nutrient poor, and are therefore expected to have room for positive social
479 interactions among microbes, potentially leading to a longer sustained beneficial effect.[68,69] In
480 the spatially structured environment, the community does not have a large impact on the
481 evolved MIC of *E. coli*. Yet, the MBC increased when the *E. coli* evolved in isolation was
482 assessed in the presence of the community. The beneficial effect of the community is therefore
483 still present even for lineages with high levels of resistance, with the exception of *E. coli*
484 evolved in the presence of the community in the well-mixed environment. This shows that the
485 beneficial effect that the community confers is not dependent on the antibiotic concentration
486 present or the fitness impact of the antibiotics on *E. coli*, but instead is dependent on the
487 evolutionary history of the *E. coli*, particularly whether it evolved within that community before.

488 The initial cell density in environments with antibiotics is important for evolutionary
489 outcomes.[16,67] In both tested environments we observed higher densities of *E. coli* when
490 embedded in the community, leading to faster evolutionary rates towards high antibiotic
491 resistance. This corresponds to the well-known inoculum effect.[15,16] Perhaps surprisingly, for
492 the *E. coli* evolved on the spatial structure in the presence of the community, this did not lead
493 to a higher MIC compared to the *E. coli* evolved in isolation (Figure 1A,B). [8]Because the MIC

494 was determined at equal population sizes of *E. coli*, this assay does not account for differences
495 in population size during the serial transfer experiments .[15] Still, indirectly, population size may
496 play a role in reaching higher MICs, because the *E. coli* with higher MICs reach larger
497 population sizes over 24 hours of growth in the absence of antibiotic. This suggests that
498 adaptation to the medium-environment contributes to the growth at higher antibiotic
499 concentrations.

500 [870]Spatial adaptation and the physical distance between interacting *E. coli* and community
501 members may play a role in the adaptation to community members. We followed the colony
502 formation in the different agar compartments (Fig S4), and did not observe any mixing of
503 colonies on that surface. From literature it is known that bacterial mobility on agar can lead to
504 a decrease in adaptation through for example increased ecological competition.[70,71] Moreover,
505 studies suggest that interactions only play a role on small scales and distances in spatially
506 structured environments,[72–74] while larger distance interactions play a role on chemotaxis of
507 bacteria.[75] These results show the difficulty of comparing spatially structured and well-mixed
508 environments, as distance dependent interactions are lost when the environment is well-
509 mixed.

510 To observe potential variation in the evolved replicates, we sequenced three clones per
511 replicate, for each of these clones we analyzed the CNVs of resistance genes and other
512 genomic changes. We also noticed many prophage mutations, particularly in the spatially
513 evolved lineages. We chose to exclude these from our H-index analysis because prophage
514 regions often evolve at different rates compared to the core bacterial genome and undergo
515 decay after integration[76], and this study aimed to compare mutations in the genome of *E. coli*
516 and its plasmid, which is more representative of the species' overall evolutionary trajectory.

517 We observed a higher number of SNPs in clones derived from the spatially structured
518 environment compared to the well-mixed environment, this was expected due to a larger effect
519 of drift in the spatial environment.[77] We also observed variability in the CNVs in some
520 replicates, for example replicate 4 in the well-mixed community environment (Figure S3),
521 seemed to have lost the plasmid containing the resistance genes, even though these
522 replicates showed high MICs. We cannot exclude that they lost their plasmids during culturing
523 for sequencing as that environment did not contain antibiotics. If this were the case, then the
524 copy number variations of the transposon on the plasmid a highly variable in time. It is also
525 possible that the observation of plasmid loss is due to high plasmid copy number segregation
526 variability, which refers to uneven distribution of plasmids during cell division and leads to
527 higher phenotypic heterogeneity, and has been observed before.[78] Moreover, insertion-
528 sequence activity and the implied mobility of the contained resistance genes could offer an

529 additional explanation for differences in the variation and observed efficacy of the resistance
530 genes. While gene copy number increases are a useful proxy for increased gene activity, gene
531 expression is key. Gene expression is influenced considerably by the location of the genes
532 within a genome and their alignment with factors regulating gene expression, such as
533 promoters. While our quantitative analysis of clonal sequencing data allows us to determine
534 gene copy numbers, it does not allow us to determine the location of any of the underlying
535 gene copies with the plasmid or host genome, and we therefore are very limited in predicting
536 the actual effect of the resistance gene copies. The potential presence of resistance plasmids
537 should be kept in mind when using sequencing techniques of clinical isolates to detect and
538 identify AMR genes, and observing where insertion sequences insert will be valuable in better
539 understanding antibiotic resistance evolution in pathogens.

540 Our investigation into the observed fluctuations in copy numbers of the plasmid carrying the
541 resistance gene, raises intriguing questions about the nuanced dynamics of antibiotic
542 resistance in microbial populations. Previous studies have underscored the complexity of
543 plasmid replication and maintenance, suggesting that various factors, including selective
544 pressures and growth rates, can influence the stability of plasmid copy numbers.[79,80] The
545 disconnect between plasmid copy numbers and MICs in our experimental context echoes
546 findings in other systems, where researchers have reported instances of decoupling between
547 plasmid abundance and phenotypic resistance[81,82]. These observations challenge
548 conventional assumptions regarding the straightforward relationship between plasmid
549 replication and antibiotic resistance expression. It is plausible that additional regulatory
550 mechanisms, such as transcriptional or post-transcriptional control, may contribute to the
551 observed variability in resistance phenotypes, such as the genomic compensatory mutations
552 related to NADH observed in the spatially-structured environment. This underscores the need
553 for comprehensive investigations into the multifaceted environmental structure, community
554 and genetic interactions governing plasmid-mediated resistance, which could provide valuable
555 insights for the development of targeted strategies to mitigate the spread of antibiotic
556 resistance in microbial communities.
557

558 **Materials and methods**

559 **Bacterial isolates and growth medium**

560 The focal *Escherichia coli* isolate and three community isolates (*Klebsiella pneumoniae*,
561 *Enterococcus faecium*, and *Staphylococcus epidermidis*) were collected anonymously in a
562 previous study from elderly patients (>70 years old) who were suffering from a urinary tract
563 infection.[37] The three community members were picked based on their ability to grow in

564 Lysogeny Broth (LB) containing 250 µg/mL trimethoprim and 1250 µg/mL sulfamethoxazole,
565 and being able to clearly distinguish all four isolates on CHROMagar Orientation
566 (CHROMagar). The *E. coli* isolate was selected based on its sensitivity to
567 trimethoprim/sulfamethoxazole. Pure cultures of each separate isolate were obtained by
568 streaking on CHROMagar plates, selecting a single colony, and growing overnight in LB broth
569 at 37°C. Overnight cultures were used to create glycerol stocks (25% glycerol v/v) which were
570 subsequently stored at -80°C. The experiments were performed in Artificial Urine Medium
571 (AUM), which is created (for a 1X concentration) by mixing 1.5 g/L bacto peptone L37 (BD),
572 3.15 g/L NaHCO3, 11.25 g/L urea (Roth), 4.8 g/L Na2SO4.10H2O, 1.8 g/L K2HPO4, 1.95 g/L
573 NH4Cl, 15 mg/L bacto yeast extract (BD), 1.98 mM lactic acid (Roth), 600 mg/L citric acid, 105
574 mg/L uric acid, 1.2 g/L creatinine, 4.44 mg/L CaCl2.2H2O, 1.8 g/L Fe(II)SO4.7H2O (Riedel),
575 368 mg/L MgSO4.7H2O, 1.43 g/L KH2PO4. Chemicals were ordered from Sigma, unless
576 stated otherwise. The pH was adjusted to 6.5 using 1M HCl. For 2x AUM, concentrations of
577 all chemicals were doubled except NaCl, which would be omitted.
578

579 **Antibiotic and X-gal stocks**

580 The trimethoprim stock was created by mixing 10 mg/mL trimethoprim in dimethyl sulfoxide
581 (DMSO), and the sulfamethoxazole stock was created by mixing 50 mg/mL sulfamethoxazole
582 in acetone. The X-gal stock contained 20 mg/mL X-Gal and 0.1M Isopropyl β-D-1-
583 thiogalactopyranoside (IPTG) mixed in DMSO. Both antibiotics, the X-gal, IPTG and solvents
584 were ordered from Sigma. The trimethoprim stock was stored at 4°C for up to two weeks, and
585 the X-gal stock and sulfamethoxazole stocks were stored at -20°C. Trimethoprim and
586 sulfamethoxazole were always mixed in a 1:5 ratio, similar to clinical settings.[38]

587 **Bacterial hotel creation and transfer protocol**

588 Silicon hotel agar molds were stored in 70% ethanol and were dried in a sterile flow cabinet
589 before pouring agar. Each agar hotel was created by mixing 12.5 mL 2x AUM, an appropriate
590 amount of antibiotics, 12.5 mL 3% soft agar in demineralized water at 60°C, and 125 µL X-
591 Gal stock for the visualization of *E. coli* into the hotel mold. Agar hotels were cooled for 30
592 minutes before removing the agar from the molds.

593 Five replicates of *E. coli* were evolved for 60 bi-daily transfers in communities with *K.*
594 *pneumoniae*, *E. faecium* and *S. epidermidis,* and in isolation. Starting cultures of all isolates
595 were created by growing each separately in 1x AUM overnight at 37°C shaken at 200 rpm.
596 Each culture was diluted a hundred times in 1x AUM. Starting agar hotels were created with
597 the starting antibiotics concentration of 50:250 µg/mL TMP:SMX. Following the layout of
598 Figure S4, 0.5 µL of each diluted culture was added to the middle of the appropriate well on

599 the agar plate. Added cultures were allowed to dry for five minutes before incubating the agar
600 hotels at 37°C for 48 hours. We did not observe any spillover of colonies to other
601 compartments.

602 Before transferring *E. coli* to a fresh agar hotel, the colonies were visibly inspected for growth.
603 If the colony's growth exceeded 1mm of the starting colony, the antibiotics concentration would
604 be increased by 20% unless the antibiotics concentration was increased during the previous
605 transfer. Exception here were the first two transfers where antibiotics were increased by 20%
606 due to clear overgrowth of *E. coli*. Replicates were transferred by streaking around the outer
607 edges of each *E. coli* colony five times and adding the bacteria that were resuspended in 50
608 µL of 1x AUM. After mixing, 0.5 µL of each replicate would be added to the fresh agar hotels.
609 Wild type community members (non-*E. coli*) were always added as hundred times diluted
610 overnight culture in 1x AUM to the fresh agar hotels.

611 **Liquid serial transfers protocol**

612 *E. coli* was evolved over 120 days in AUM transferring replicates to fresh 5 mL medium every
613 48 hours for 60 transfers in total. To start, the *E. coli* and the three community members were
614 streaked on agar to obtain a pure culture of a single colony that was cultured overnight in AUM
615 at 37°C, shaken at 200 rpm. Isolates were diluted a hundred times by adding 50 µL to 5mL
616 total preheated medium. Five replicates of *E. coli* in isolation and five replicates of *E. coli* with
617 the three community members *K. pneumoniae, E. faecium*, and *S. epidermidis*. An appropriate
618 amount of the antibiotics were added to the medium before adding the bacteria. Antibiotic
619 concentration started at 50:250 µg/mL TMP:SMX. Cultures were allowed to grow for 48 hours
620 at 37°C and shaken at 200 rpm. During transfer, the previous culture was diluted a hundred
621 times and community members were added fresh. Remaining culture was used to do colony
622 counting measurements on CHROMagar plates to obtain a CFU/mL count for *E. coli*. If *E. coli*
623 had exceeded $1*10^6$ CFU/mL, antibiotic concentration would be increased by 20% for the next
624 transfer. For the first two transfers for *E. coli* evolving in presence of the community, the
625 antibiotic concentration was increased by 20% immediately due to observed high population
626 growth based on turbidity.

627 **MIC and MBC assays**

628 MIC of replicates were measured in liquid using a two times serial dilution of antibiotics
629 method. Using the concentration of antibiotics at the final transfer step as a guideline, a dilution
630 series was created for each isolate specifically. Measurements were performed in 96-well
631 microtiter plates, using AUM as growth medium. Stationary phase cultures of *E. coli* replicates
632 were used for experiments, diluting them 40x times in the medium antibiotics' mixture. Plates
633 were incubated overnight at 37°C, shaken at 200 rpm. Growth was measured through

634 absorbance at 600nm using a BMG CLARIOstar microplate reader. If the absorbance with the
635 background subtracted exceeded 0.1, it was assumed that *E. coli* had grown using the lowest
636 concentration of antibiotics where no growth was observed is the MIC. All MIC measurements
637 were performed in triplicate.
638
639 MBC assays with community present were performed following the above protocol, but with
640 community members added together with the *E. coli* before overnight growth. After OD600
641 measurements, presence of *E. coli* was confirmed using a 96-well pinning tool on
642 CHROMagar. The lowest concentration of antibiotics where no growth of E.coli on
643 CHROMagar was observed is the MBC.

644

645 **DNA extraction and sequencing**

646 DNA from first transfer clones and final transfer mutants were extracted using the QIAamp
647 DNA Mini Kit (Qiagen, Hilden, Germany) following the manufacturer's instructions. DNA was
648 eluted in 100 µL elution buffer AE. Quality and quantity of isolated DNA were checked using
649 a Nanodrop One^{C} Microvolume UV-Vis Spectrophotometer (Thermo Fisher Scientific, USA).

650 Three clones of the final transfer step for each of the five replicate lineages per experimental
651 setting were sent for illumina sequencing at SeqCenter (Pittsburgh, PA, USA). Five replicates
652 of community members isolated from *E. coli* community agar and liquid were also sent to
653 SeqCenter, Pittsburgh, USA for Illumina sequencing.

654 Illumina sequencing libraries were prepared using the tagmentation-based and PCR-based
655 Illumina DNA Prep kit and custom IDT 10bp unique dual indices (UDI) with a target insert size
656 of 320 bp. No additional DNA fragmentation or size selection steps were performed. Illumina
657 sequencing was performed on an Illumina NovaSeq 6000 sequencer in one or more
658 multiplexed shared-flow-cell runs, producing 2x151bp paired-end reads. Demultiplexing,
659 quality control and adapter trimming was performed with bcl-convert1 (v4.1.5). In total 10.9
660 Gbp and 359.2 Gbp of read data were produced from ancestral and evolved strains,
661 respectively.

662 Ancestor strains were sent to the same company for Nanopore sequencing. Sample libraries
663 were prepared using Oxford Nanopore Technologies (ONT) Ligation Sequencing Kit (SQK-
664 NBD114.24) with NEBNext® Companion Module (E7180L) to manufacturer's specifications.
665 All samples were run on Nanopore R10.4.1 flow cells and MinION Mk1B device. Post-
666 sequencing, Guppy (v6.3.8) was used for super high accuracy base calling (SUP) and
667 demultiplexing. Overall, 2.9 Gbp of read data were produced.

668 **Genome assembly, annotation variant calling and effect prediction**

669 The wildtype reference assembly was generated with flye v2.9.2 (settings: --nano-hq)[83] from
670 the ancestral nanopore data and polished using ancestral Illumina read with polca.sh included
671 in the MaSuRCA v4.1.0 Genome Assembly and Analysis Toolkit.[84] Genes were annotated
672 with Bakta v1.8.1[85] and integrated prophages and plasmids with genomad v1.7.4[86] for each
673 replicate were called from read mappings generated with minimap2 v2.26[87] using freebayes
674 v1.3.1 (settings: -p 1 -0 -F 0.5)[88] and filtered for spurious calls with bcftools v1.17 (--exclude
675 'REF~"N" || QUAL < 20 || INFO/DP < 10').[89] Variant effects were predicted with the Ensembl
676 Variant Effect Predictor (VEP) v110.1 command line tool.

677 ***H*-index calculation**

678 To quantify the repeatability of mutations within our *E. coli* mutants, the *H*-index of genome
679 repeatability previously described by Schenk et al. was calculated.[50] The *H*-index was
680 calculated on the functional (COG) and at the gene level. All mutant replicates were compared
681 pairwise, each one-way comparison calculated using:

682 $$H_{A,B} = \sum_{j=1}^{m}\sum_{k=1}^{n}\left(\frac{|A_j \cap B_k|}{|A_j|}\right) / \sum_{j=1}^{m}\sum_{k=1}^{m}\left(\frac{|A_j \cap A_l|}{|A_j|}\right) \quad (1)$$

683 In the formula (1), genotype A and B with mutations m and n respectively are compared. The
684 final *H*-index of the combination is obtained for both genotypes separately ($H_{A,B}$ and $H_{B,A}$) and
685 compared using:

686 $$H = \frac{H_{A,B} + H_{B,A}}{2} \quad (2)$$

687 The final *H*-index value falls between 0 (no repeated evolution) and 1 (complete parallelism).
688 An *H*-index value of 0.5 indicates that the average of the two compared mutants have half of
689 their mutations shared between them.

690 **Statistical analysis**

691 When comparing the values between two conditions of mutants, a two-tailed *Welch's t*-test
692 was performed to test the null hypothesis that the two parameters do not have significantly
693 different values (hypothesis of neutrality). To determine level of correlation between two
694 variables, we used the square of a Pearsson correlation coefficient and resulting *P*-value
695 where the null-hypothesis was rejected with a significance level above 0.05. For multiple
696 pairwise comparisons, we used independent sample *t*-tests for all sets with a Bonferroni-
697 correction to adjust *P*-values to reduce type I errors.

698

699

Author contribution

Conceived and designed the study: LEZ MGJDV. Performed the experiments: LEZ MB JML. Analyzed the data: LEZ TH MGJ. Wrote the manuscript: LEZ JML TH MGJ.

Acknowledgements

LEZ was supported by the Adaptive Life program of the Faculty of Science and Engineering, within GELIFES. MB was supported by the Faculty of Science and Engineering - Adaptive Life PhD Scholarship from the University of Groningen, awarded by GELIFES.

709 **References**

710

711 1 Byrd AL, Segre JA. Adapting Koch's postulates: Criteria for disease causation must
712 take microbial interactions into account. *Science (1979)* 2016; **351**: 224–226.

713 2 Peters BM, Jabra-Rizk MA, O'May GA, William Costerton J, Shirtliff ME. Polymicrobial
714 interactions: Impact on pathogenesis and human disease. *Clin Microbiol Rev* 2012;
715 **25**: 193–213.

716 3 Gaston JR, Johnson AO, Bair KL, White AN, Armbruster CE. Polymicrobial
717 interactions in the urinary tract: Is the enemy of my enemy my friend? *Infect Immun*
718 2021; **89**. doi:10.1128/IAI.00652-20.

719 4 Zandbergen LE, Halverson T, Brons JK, Wolfe AJ, de Vos MGJ. The Good and the
720 Bad: ecological interaction measurements between the urinary microbiota and
721 uropathogens. *Front Microbiol* 2021; **12**: 659450.

722 5 Short FL, Murdoch SL, Ryan RP. Polybacterial human disease: The ills of social
723 networking. *Trends Microbiol* 2014; **22**: 508–516.

724 6 Vega NM, Gore J. Collective antibiotic resistance: Mechanisms and implications. *Curr*
725 *Opin Microbiol* 2014; **21**: 28–34.

726 7 Bottery MJ, Pitchford JW, Friman VP. Ecology and evolution of antimicrobial
727 resistance in bacterial communities. *ISME Journal* 2021; **15**: 939–948.

728 8 Klümper U, Recker M, Zhang L, Yin X, Zhang T, Buckling A *et al.* Selection for
729 antimicrobial resistance is reduced when embedded in a natural microbial community.
730 *ISME Journal* 2019; **13**: 2927–2937.

731 9 Algammal A, Hetta HF, Mabrok M, Behzadi P. Editorial: Emerging multidrug-resistant
732 bacterial pathogens "superbugs": A rising public health threat. *Front Microbiol* 2023;
733 **14**. doi:10.3389/fmicb.2023.1135614.

734 10 De Vos MGJ, Zagorski M, McNally A, Bollenbach T. Interaction networks, ecological
735 stability, and collective antibiotic tolerance in polymicrobial infections. *Proc Natl Acad*
736 *Sci U S A* 2017; **114**: 10666–10671.

737 11 Geyrhofer L, Ruelens P, Farr AD, Pesce D, de Visser JAGM, Brenner N. Minimal
738 surviving inoculum in collective antibiotic resistance. *mBio* 2023; **14**.
739 doi:10.1128/mbio.02456-22.

740 12 Biswas L, Biswas R, Schlag M, Bertram R, Götz F. Small-colony variant selection as a
741 survival strategy for Staphylococcus aureus in the presence of *Pseudomonas*
742 *aeruginosa*. *Appl Environ Microbiol* 2009; **75**: 6910–6912.

743 13 Brauner A, Fridman O, Gefen O, Balaban NQ. Distinguishing between resistance,
744 tolerance and persistence to antibiotic treatment. *Nat Rev Microbiol* 2016; **14**: 320–
745 330.

746 14 Zandbergen LE, van den Heuvel J, Farr AD, Zwaan BJ, de Visser JAGM, de Vos
747 MGJ. Microbial interactions affect the tempo and mode of antibiotic resistance
748 evolution. *bioRxiv* 2024; 2024.06.06.597700.

749 15 Brook I. Inoculum Effect. *Rev Infect Dis* 1989; **11**: 361–368.

750 16 Tan C, Phillip Smith R, Srimani JK, Riccione KA, Prasada S, Kuehn M *et al.* The
751 inoculum effect and band-pass bacterial response to periodic antibiotic treatment. *Mol*
752 *Syst Biol* 2012; **8**. doi:10.1038/msb.2012.49.

753 17 Foster KR, Bell T. Competition, not cooperation, dominates interactions among
754 culturable microbial species. *Current Biology* 2012; **22**: 1845–1850.

755 18 Lee J-H, Lee J. Indole as an intercellular signal in microbial communities. *FEMS*
756 *Microbiol Rev* 2010; **34**: 426–444.

757 19 Flemming HC, Wingender J, Szewzyk U, Steinberg P, Rice SA, Kjelleberg S. Biofilms:
758 An emergent form of bacterial life. *Nat Rev Microbiol* 2016; **14**: 563–575.

759 20 Costerton JW, Stewart PS, Greenberg. Bacterial biofilms: a common cause of
760 persistant infections. *Science (1979)* 1999; **284**: 1318–1322.

761 21 Dieckmann U, Law R, Metz JAJ. *The Geometry of Ecological Interactions: Simplifying*
762 *Spatial Complexity*. Cambridge University Press, 2002 doi:10.1016/s0925-
763 8574(01)00102-1.

764 22 Tilman D, Kareiva P. *Spatial Ecology: The Role of Space in Population Dynamics and*
765 *Interspecific Interactions. David Tilman , Peter Kareiva*. Princeton University Press,
766 1998 doi:10.1086/420507.

767 23 Johnson CR, Seinen I. Selection for restraint in competitive ability in spatial
768 competition systems. *Proceedings of the Royal Society B: Biological Sciences* 2002;
769 **269**: 655–663.

770 24 Kerr B, Riley MA, Feldman MW, Bohannan BJM. Local dispersal promotes
771 biodiversity in a real-life game of rock-paper-scissors. *Nature* 2002; **418**: 171–174.

772 25 Yanni D, Márquez-Zacarías P, Yunker PJ, Ratcliff WC. Drivers of Spatial Structure in
773 Social Microbial Communities. *Current Biology* 2019; **29**: R545–R550.

774 26 Evans KC, Benomar S, Camuy-Vélez LA, Nasseri EB, Wang X, Neuenswander B *et*
775 *al.* Quorum-sensing control of antibiotic resistance stabilizes cooperation in
776 *Chromobacterium violaceum*. *ISME J* 2018; **12**: 1263–1272.

777 27 Chuang SK, Vrla GD, Fröhlich KS, Gitai Z. Surface association sensitizes
778 Pseudomonas aeruginosa to quorum sensing. *Nat Commun* 2019; **10**: 4118.

779 28 Nowak MA, May RM. Evolutionary games and spatial chaos. *Nature* 1992; **359**: 826–
780 829.

781 29 Santos FC, Pacheco JM, Lenaerts T. Evolutionary dynamics of social dilemmas in
782 structured heterogeneous populations. *Proc Natl Acad Sci U S A* 2006; **103**: 3490–
783 3494.

784 30 Nadell CD, Drescher K, Foster KR. Spatial structure, cooperation and competition in
785 biofilms. Nat Rev Microbiol. 2016; **14**: 589–600.

786 31 Verbruggen E, El Mouden C, Jansa J, Akkermans G, Bücking H, West SA *et al.*
787 Spatial structure and interspecific cooperation: Theory and an empirical test using the
788 mycorrhizal mutualism. *American Naturalist* 2012; **179**: E133-46.

789 32 Bailey SF, Trudeau A, Tulowiecki K, McGrath M, Belle A, Fountain H *et al.* Spatial
790 structure affects evolutionary dynamics and drives genomic diversity in experimental
791 populations of *Pseudomonas fluorescens*. 2021. doi:10.1101/2021.09.28.461808.

792 33 Lobanov A, Dyckman S, Kurkjian H, Momeni B. Spatial structure favors microbial
793 coexistence except when slower mediator diffusion weakens interactions. *Elife* 2023;
794 **12**. doi:10.7554/eLife.82504.

795 34 Momeni B, Waite AJ, Shou W. Spatial self-organization favors heterotypic cooperation
796 over cheating. *Elife* 2013; **2**. doi:10.7554/eLife.00960.

797 35 Habets MGJL, Rozen DE, Hoekstra RF, De Visser JAGM. The effect of population
798 structure on the adaptive radiation of microbial populations evolving in spatially
799 structured environments. *Ecol Lett* 2006; **9**: 1041–1048.

800 36 Perfeito L, Pereira MI, Campos PR, Gordo I. The effect of spatial structure on
801 adaptation in Escherichia coli. *Biol Lett* 2008; **4**: 57–59.

802 37 Croxall G, Weston V, Joseph S, Manning G, Cheetham P, McNally A. Increased
803 human pathogenic potential of Escherichia coli from polymicrobial urinary tract

804 infections in comparison to isolates from monomicrobial culture samples. *J Med*
805 *Microbiol* 2011; **60**: 102–109.

806 38 Hitchings GH. Mechanism of action of trimethoprim-sulfamethoxazole--I. *J Infect Dis*
807 1973; **128**: S433.

808 39 Mann R, Mediati DG, Duggin IG, Harry EJ, Bottomley AL. Metabolic adaptations of
809 Uropathogenic E. coli in the urinary tract. *Front Cell Infect Microbiol* 2017; **7**.
810 doi:10.3389/fcimb.2017.00241.

811 40 Webb CO, Ackerly DD, McPeek MA, Donoghue MJ. Phylogenies and community
812 ecology. *Annu Rev Ecol Syst* 2002; **33**: 475–505.

813 41 Geisinger E, Isberg RR. Antibiotic Modulation of Capsular Exopolysaccharide and
814 Virulence in Acinetobacter baumannii. *PLoS Pathog* 2015; **11**: e1004691.

815 42 Santos-Lopez A, Marshall CW, Scribner MR, Snyder DJ, Cooper VS. Evolutionary
816 pathways to antibiotic resistance are dependent upon environmental structure and
817 bacterial lifestyle. *Elife* 2019; **8**. doi:10.7554/elife.47612.

818 43 Brockhurst MA, Habets MGJL, Libberton B, Buckling A, Gardner A. Ecological drivers
819 of the evolution of public-goods cooperation in bacteria. *Ecology* 2010; **91**: 334–340.

820 44 Tamer YT, Gaszek IK, Abdizadeh H, Batur TA, Reynolds KA, Atilgan AR *et al.* High-
821 order epistasis in catalytic power of dihydrofolate reductase gives rise to a rugged
822 fitness landscape in the presence of trimethoprim selection. Mol Biol Evol. 2019; **36**:
823 1533–1550.

824 45 Vedantam G, Guay GG, Austria NE, Doktor SZ, Nichols BP. Characterization of
825 mutations contributing to sulfathiazole resistance in Escherichia coli. *Antimicrob*
826 *Agents Chemother* 1998; **42**: 88–93.

827 46 Liebert CA, Hall RM, Summers AO. Transposon Tn 21 , Flagship of the Floating
828 Genome . *Microbiology and Molecular Biology Reviews* 1999; **63**: 507–522.

829 47 San Millan A, MacLean RC. Fitness Costs of Plasmids: a Limit to Plasmid
830 Transmission. *Microbiol Spectr* 2017; **5**. doi:10.1128/microbiolspec.mtbp-0016-2017.

831 48 Dimitriu T, Matthews AC, Buckling A. Increased copy number couples the evolution of
832 plasmid horizontal transmission and plasmid-encoded antibiotic resistance. *Proc Natl*
833 *Acad Sci U S A* 2021; **118**: e2107818118.

834 49 Hallatschek O, Hersen P, Ramanathan S, Nelson DR. Genetic drift at expanding
835 frontiers promotes gene segregation. *Proc Natl Acad Sci U S A* 2007; **104**: 19926–
836 19930.

837 50 Schenk MF, Zwart MP, Hwang S, Ruelens P, Severing E, Krug J *et al.* Population size
838 mediates the contribution of high-rate and large-benefit mutations to parallel evolution.
839 Nat Ecol Evol. 2022; **6**: 439–447.

840 51 Buwembo W, Aery S, Rwenyonyi CM, Swedberg G, Kironde F. Point mutations in the
841 folP gene partly explain sulfonamide resistance of streptococcus mutans. *Int J*
842 *Microbiol* 2013; **2013**: 367021.

843 52 Rimmele M, Boos W. Trehalose-6-phosphate hydrolase of Escherichia coli. *J*
844 *Bacteriol* 1994; **176**: 5654–5664.

845 53 Botelho J, Schulenburg H. The Role of Integrative and Conjugative Elements in
846 Antibiotic Resistance Evolution. *Trends Microbiol* 2021; **29**: 8–18.

847 54 Amro J, Baron C. TraC of the conjugative plasmid pKM101 is secreted as a monomer
848 in outer membrane vesicles and stimulates conjugation. *bioRxiv* 2022; : 2022–2027.

849 55 Nakayama J, Takanami Y, Horii T, Sakuda S, Suzuki A. Molecular Mechanism of
850 Peptide-Specific Pheromone Signaling in *Enterococcus faecalis* : Functions of
851 Pheromone Receptor TraA and Pheromone-Binding Protein TraC Encoded by
852 Plasmid pPD1. *J Bacteriol* 1998; **180**: 449–456.

853 56 Cho H, Winans SC. TraA, TraC and TraD autorepress two divergent quorum-
854 regulated promoters near the transfer origin of the Ti plasmid of *Agrobacterium*
855 *tumefaciens*. *Mol Microbiol* 2007; **63**: 1769–1782.

856 57 Parvathy ST, Udayasuriyan V, Bhadana V. Codon usage bias. *Mol Biol Rep* 2022; **49**:
857 539–565.

858 58 Mengin-Lecreulx D, van Heijenoort J, Park JT. Identification of the mpl gene encoding
859 UDP-N-acetylmuramate: L-alanyl-gamma-D-glutamyl-meso-diaminopimelate ligase in
860 Escherichia coli and its role in recycling of cell wall peptidoglycan. *J Bacteriol* 1996;
861 **178**: 5347–5352.

862 59 Vinopal RT, Clifton D, Fraenkel DG. PfkA locus of Escherichia coli. *J Bacteriol* 1975;
863 **122**: 1162–1171.

60 Siedler S, Bringer S, Bott M. Increased NADPH availability in *Escherichia coli*: improvement of the product per glucose ratio in reductive whole-cell biotransformation. *Appl Microbiol Biotechnol* 2011; **92**: 929–937.

61 Gerasimova AV, Gelfand MS. Evolution of the Nadr regulon in enterobacteriaceae. *J Bioinform Comput Biol* 2005; **03**: 1007–1019.

62 Tritz GJ, Chandler JL. Recognition of a Gene Involved in the Regulation of Nicotinamide Adenine Dinucleotide Biosynthesis. *J Bacteriol* 1973; **114**: 128–136.

63 Arce-Rodríguez A, Pankratz D, Preusse M, Nikel PI, Häussler S. Dual Effect: high NADH levels contribute to efflux-mediated antibiotic resistance but drive lethality mediated by reactive oxygen species. *mBio* 2022; **13**. doi:10.1128/mbio.02434-21.

64 Kessler D, Leibrecht I, Knappe J. Pyruvate-formate-lyase-deactivase and acetyl-CoA reductase activities of *Escherichia coli* reside on a polymeric protein particle encoded by *adhE*. *FEBS Lett* 1991; **281**: 59–63.

65 Krucinska J, Lombardo MN, Erlandsen H, Estrada A, Si D, Viswanathan K *et al.* Structure-guided functional studies of plasmid-encoded dihydrofolate reductases reveal a common mechanism of trimethoprim resistance in Gram-negative pathogens. *Commun Biol* 2022; **5**: 459.

66 Tenaillon O, Rodríguez-Verdugo A, Gaut RL, McDonald P, Bennett AF, Long AD *et al.* The molecular diversity of adaptive convergence. *Science (1979)* 2012; **335**: 457–461.

67 Yurtsev EA, Chao HX, Datta MS, Artemova T, Gore J. Bacterial cheating drives the population dynamics of cooperative antibiotic resistance plasmids. *Mol Syst Biol* 2013; **9**: 683.

68 Piccardi P, Vessman B, Mitri S. Toxicity drives facilitation between 4 bacterial species. *Proceedings of the National Academy of Sciences* 2019; **116**: 15979–15984.

69 Adamowicz EM, Muza M, Chacón JM, Harcombe WR. Cross-feeding modulates the rate and mechanism of antibiotic resistance evolution in a model microbial community of Escherichia coli and Salmonella enterica. *PLoS Pathog* 2020; **16**: e1008700.

70 Butler MT, Wang Q, Harshey RM. Cell density and mobility protect swarming bacteria against antibiotics. *Proc Natl Acad Sci U S A* 2010; **107**: 3776–3781.

71 Piskovsky V, Oliveira NM. Bacterial motility can govern the dynamics of antibiotic resistance evolution. *Nat Commun* 2023; **14**: 5584.

896 72 Keogh D, Tay WH, Ho YY, Dale JL, Chen S, Umashankar S *et al.* Enterococcal
897 Metabolite Cues Facilitate Interspecies Niche Modulation and Polymicrobial Infection.
898 *Cell Host Microbe* 2016; **20**: 493–503.

899 73 Co AD, van Vliet S, Kiviet DJ, Schlegel S, Ackermann M. Short-range interactions
900 govern the dynamics and functions of microbial communities. *Nat Ecol Evol* 2020; **4**:
901 366–375.

902 74 van Tatenhove-Pel RJ, Rijavec T, Lapanje A, van Swam I, Zwering E, Hernandez-
903 Valdes JA *et al.* Microbial competition reduces metabolic interaction distances to the
904 low µm-range. *ISME Journal* 2021; **15**: 688–701.

905 75 Stocker R, Seymour JR. Ecology and Physics of Bacterial Chemotaxis in the Ocean.
906 *Microbiology and Molecular Biology Reviews* 2012; **76**: 792–812.

907 76 Canchaya C, Proux C, Fournous G, Bruttin A, Brüssow H. Prophage genomics.
908 *Microbiol Mol Biol Rev* 2003; **67**: 238–76, table of contents.

909 77 Zhang Q, Lambert G, Liao D, Kim H, Robin K, Tung CK *et al.* Acceleration of
910 emergence of bacterial antibiotic resistance in connected microenvironments. *Science*
911 *(1979)* 2011; **333**: 1764–1767.

912 78 Hernandez-Beltran JCR, Rodríguez-Beltrán J, Aguilar-Luviano OB, Velez-Santiago J,
913 Mondragón-Palomino O, MacLean RC *et al.* Plasmid-mediated phenotypic noise
914 leads to transient antibiotic resistance in bacteria. *Nat Commun* 2024; **15**: 2610.

915 79 Baltrus DA. Exploring the costs of horizontal gene transfer. *Trends Ecol Evol* 2013;
916 **28**: 489–495.

917 80 Millan AS, Santos-Lopez A, Ortega-Huedo R, Bernabe-Balas C, Kennedy SP,
918 Gonzalez-Zorn B. Small-plasmid-mediated antibiotic resistance is enhanced by
919 increases in plasmid copy number and bacterial fitness. *Antimicrob Agents*
920 *Chemother* 2015; **59**: 3335–3341.

921 81 Bouma JE, Lenski RE. Evolution of a bacteria/plasmid association. *Nature* 1988; **335**:
922 351–352.

923 82 Stokes HW, Gillings MR. Gene flow, mobile genetic elements and the recruitment of
924 antibiotic resistance genes into Gram-negative pathogens. *FEMS Microbiol Rev* 2011;
925 **35**: 790–819.

926 83 Kolmogorov M, Yuan J, Lin Y, Pevzner PA. Assembly of long, error-prone reads using
927 repeat graphs. *Nat Biotechnol* 2019; **37**: 540–546.

928 84 Zimin A V., Puiu D, Luo M-C, Zhu T, Koren S, Marçais G *et al.* Hybrid assembly of the
929 large and highly repetitive genome of *Aegilops tauschii* , a progenitor of bread wheat,
930 with the MaSuRCA mega-reads algorithm. *Genome Res* 2017; **27**: 787–792.

931 85 Schwengers O, Jelonek L, Dieckmann MA, Beyvers S, Blom J, Goesmann A. Bakta:
932 rapid and standardized annotation of bacterial genomes via alignment-free sequence
933 identification. *Microb Genom* 2021; **7**. doi:10.1099/mgen.0.000685.

934 86 Camargo AP, Roux S, Schulz F, Babinski M, Xu Y, Hu B *et al.* Identification of mobile
935 genetic elements with geNomad. *Nat Biotechnol* 2024; **42**: 1303–1312.

936 87 Li H. Minimap2: pairwise alignment for nucleotide sequences. *Bioinformatics* 2018;
937 **34**: 3094–3100.

938 88 Garrison E, Marth G. Haplotype-based variant detection from short-read sequencing.
939 2012.

940 89 Danecek P, Bonfield JK, Liddle J, Marshall J, Ohan V, Pollard MO *et al.* Twelve years
941 of SAMtools and BCFtools. *Gigascience* 2021; **10**. doi:10.1093/gigascience/giab008.

942

943

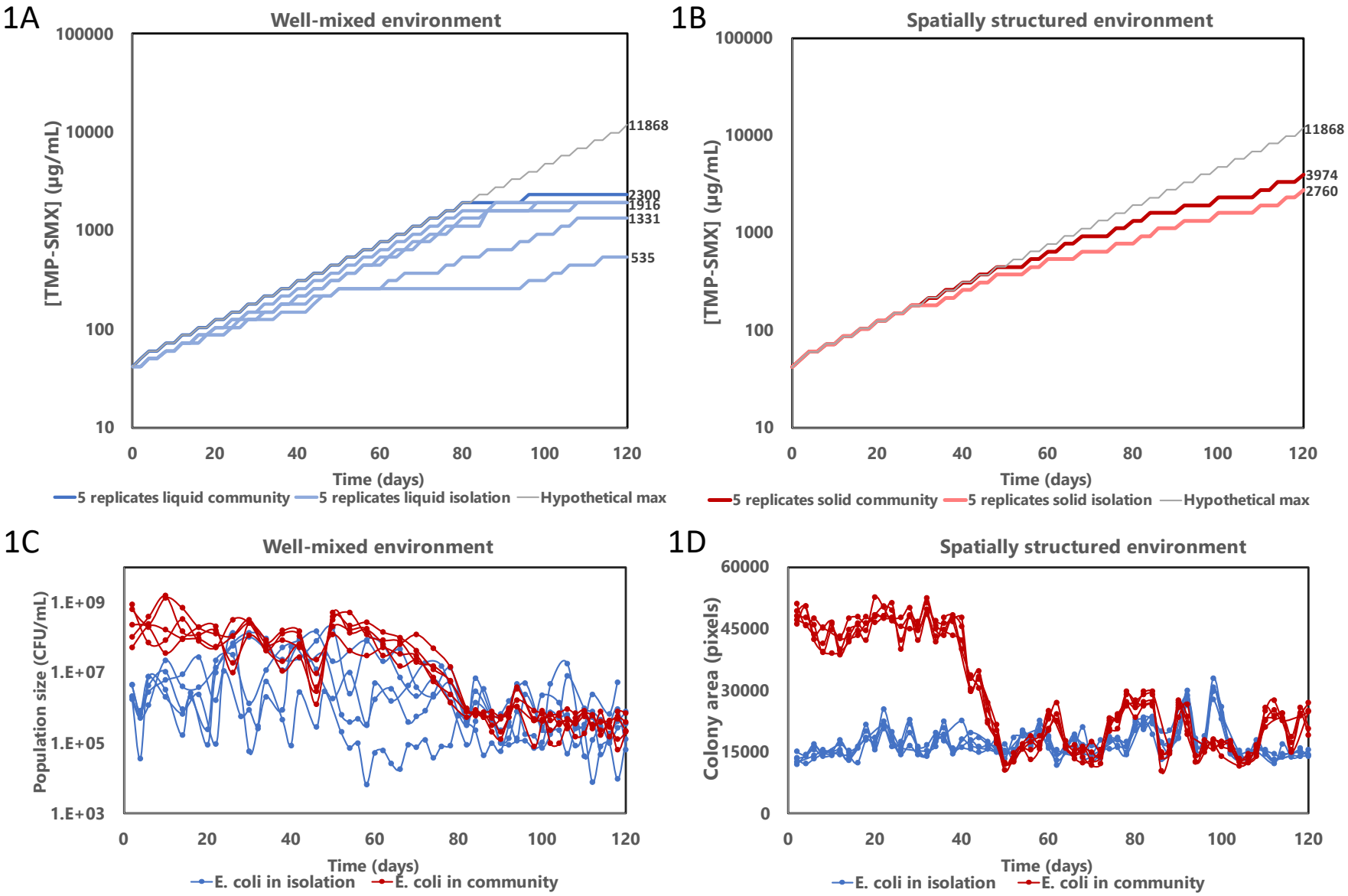
1A
Well-mixed environment
[TMP-SMX] (µg/mL)
100000
10000
1000
100
10
0
20
40
60
80
100
120
Time (days)
11868
2300
1916
1331
535
5 replicates liquid community
5 replicates liquid isolation
Hypothetical max
1B
Spatially structured environment
[TMP-SMX] (µg/mL)
100000
10000
1000
100
10
0
20
40
60
80
100
120
Time (days)
11868
3974
2760
5 replicates solid community
5 replicates solid isolation
Hypothetical max
1C
Well-mixed environment
Population size (CFU/mL)
1.E+09
1.E+07
1.E+05
1.E+03
0
20
40
60
80
100
120
Time (days)
E. coli in isolation
E. coli in community
1D
Spatially structured environment
Colony area (pixels)
60000
45000
30000
15000
0
0
20
40
60
80
100
120
Time (days)
E. coli in isolation
E. coli in community

Figure 1 | Phentoypic trajectories of trimethoprim-sulfamethoxazole antibiotic resistance evolution and population sizes of *E. coli* over time. *E. coli* evolved in the presence and absence of a community, consisting of *Klebsiella pneumoniae*, *Enterococcus faecium* and *Staphylococcus epidermidis*. *E. coli* was evolved in presence of trimethoprim-sulfamethoxazole (TMP-SMX) at a 1:5 ratio. Each condition was replicated five times. **AB,** concentration of TMP-SMX in the medium for all evolving replicate lineages within the well-mixed liquid environment (A) and spatially structured environment (B) over time. Concentrations of TMP-SMX are given by the trimethoprim concentrations. All five replicate lineages converged and overlapped for *E. coli* evolving in the presence of the community, for both well-mixed spatially structured environments. Different trajectories can be observed for *E. coli* evolving in the absence of the community within the well-mixed liquid environment. **C,** population size of *E. coli* in the well-mixed liquid environment in CFU/mL. A decline of the *E. coli* population size evolved in the presence of the community can be observed after fifty days, for all five replicate lineages. The population size of *E. coli* evolving in isolation showed large fluctuations in the first eighty days, these became less diverse after this time. **D,** population size of *E. coli* evolved in the spatially structured solid environment measured as colony area in pixels. A clear decline of colony size for *E. coli* evolved in the presence of the community can be observed after roughly forty days for all five

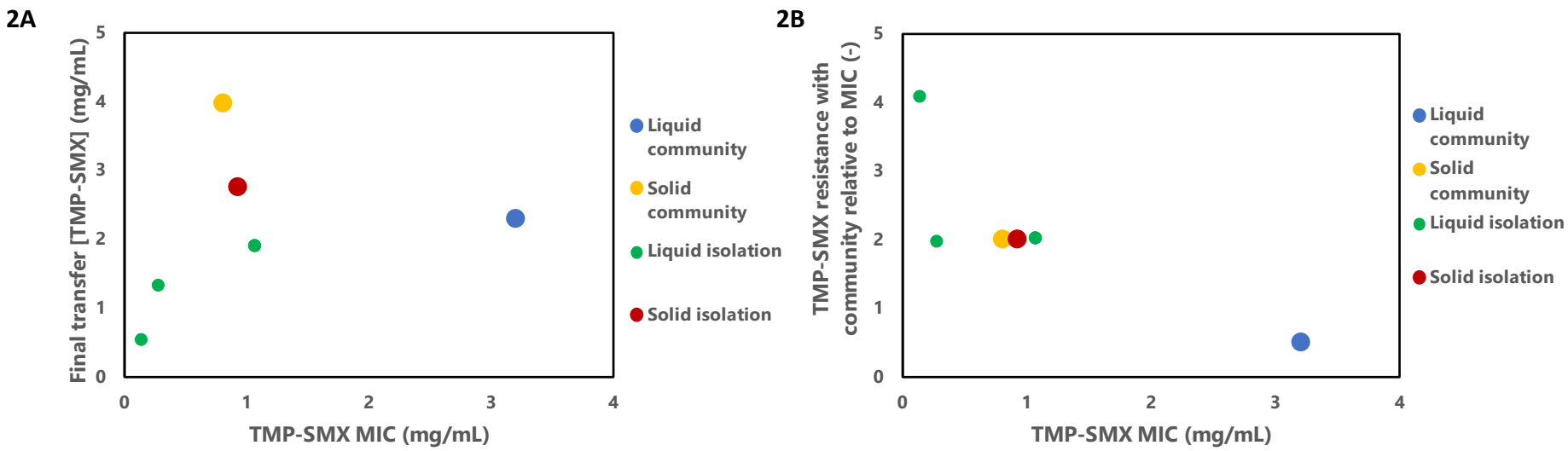

Figure 2 | Relationship between the minimal inhibitory concentration (MIC) of evolved clones, in the presence and absence of the community, and the antibiotic concentrations at final transfer. The size of the data points shows the number of replicates, with the smallest data point being one replicate and the largest all five replicates. *E. coli* was evolved in presence of trimethoprim-sulfamethoxazole (TMP-SMX) at a 1:5 ratio. Concentrations of TMP-SMX are given by the trimethoprim concentrations. **A,** MIC of evolved *E.coli* versus the concentration of antibiotic at the final transfer step at day 120. No clear correlation between the MIC of evolved clones, and the concentration of antibiotic in the medium at their final transfer could be observed. **B,** MIC of evolved *E.coli* versus the community effect on MIC. The community resistance effect was determined by performing an MBC assay in the presence of the community, followed by subsequent transfer on agar. The concentration of trimethoprim-sulfamethoxazole at which no *E. coli* could be observed on the agar, is given relative to the MBC of *E. coli* in isolation. Therefore, a value above 1 on the y-axis indicates a higher observed resistance compared to measured MIC, while a value below 1 indicates a low resistance compared to the MIC. Only *E. coli* evolved in liquid medium in the presence of the community did not benefit from the presence of the community in the community MBC assay (blue). Absolute resistance levels in the presence of community are depicted in Figure S1.

3A

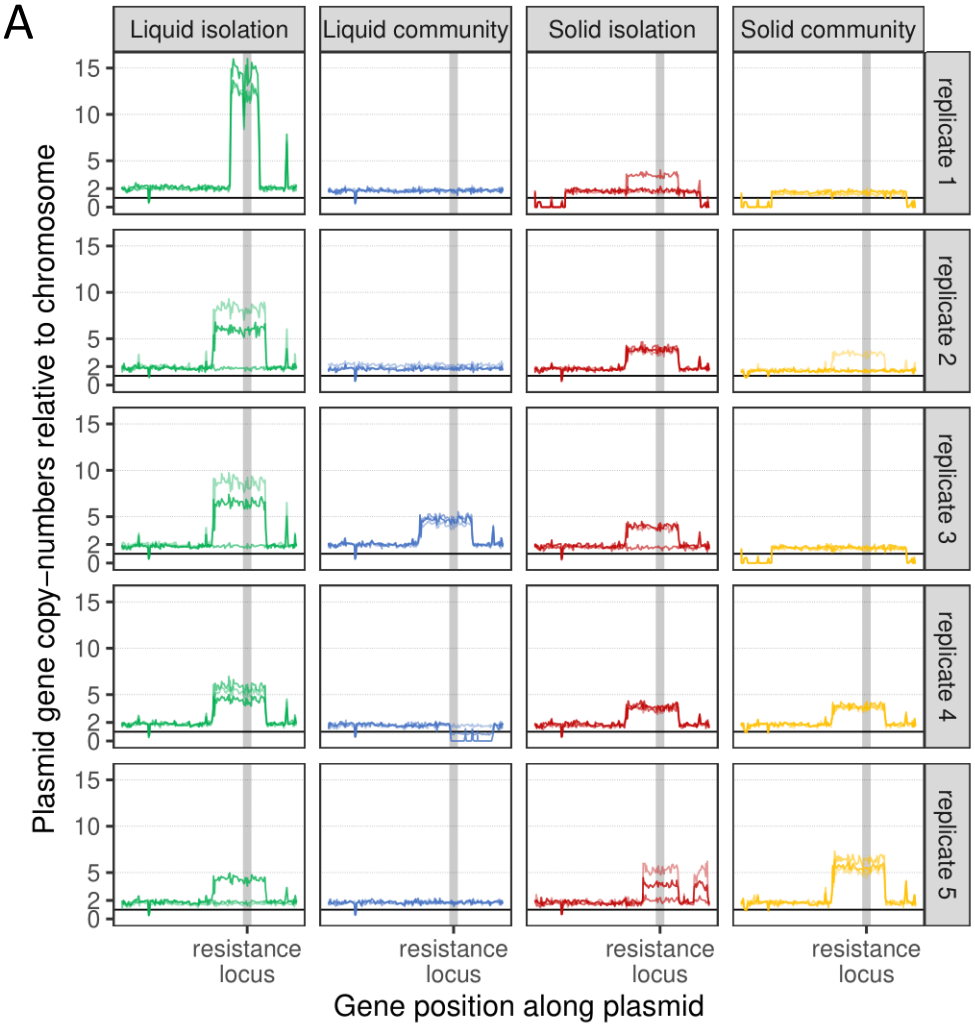
Liquid isolation
Liquid community
Solid isolation
Solid community
replicate 1
replicate 2
replicate 3
replicate 4
replicate 5
Plasmid gene copy−numbers relative to chromosome
15
10
5
2
0
resistance locus
Gene position along plasmid

3B

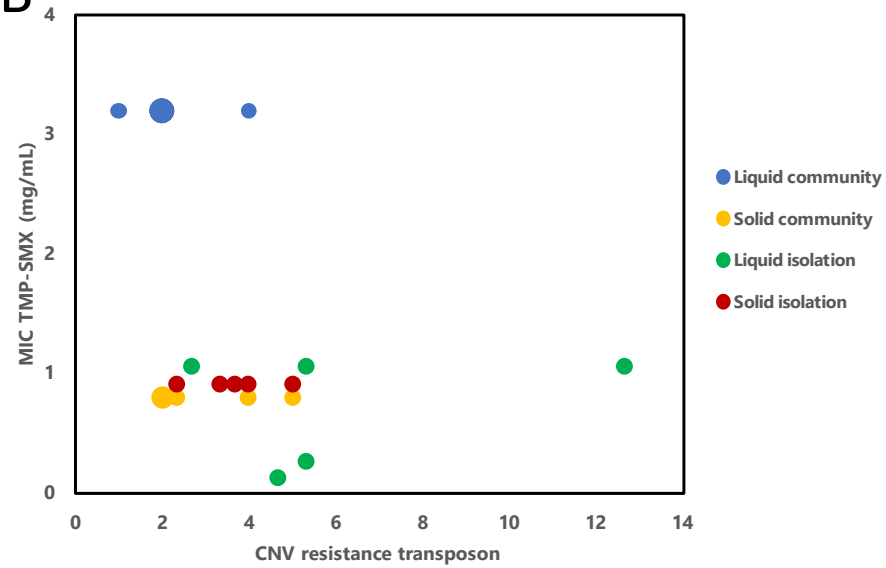
MIC TMP-SMX (mg/mL)
CNV resistance transposon
0
1
2
3
4
0
2
4
6
8
10
12
14
Liquid community
Solid community
Liquid isolation
Solid isolation

Figure 3 | Copy number variation in the plasmid containing the antibiotic resistance genes in the final transfer mutants. Three clones were sequenced per replicate, showing genetic copy number variation within the population. **A.** Copy number variation in the TN21-like integron cassette part of the plasmid containing *dfrA17* and *sul1,* which confer resistance to trimethoprim and sulfamethoxazole, respectively, in each of the sequenced clones. The highlighted region in gray contains the resistance genes, showing overall a tendency for increased copy numbers of this region. Some replicates do not have increased copy numbers of the resistance genes compared to the wild type. Particularly those evolved in the liquid environment in the presence of the community (blue), and in the solid spatially structured environment in the presence of the community (yellow). **B.** Average copy number variation per replicate in the TN21-like integron cassette part of the plasmid containing *dfrA17* and *sul1* resistance genes versus resistance level (MIC) of evolved replicate lineages. Concentrations of trimethoprim-sulfamethoxazole (1:5 ratio) are given by the trimethoprim concentrations. No clear pattern between replicates evolved in the same environment could be observed. Copy number variation for each sequenced clone is depicted in Figure S3.

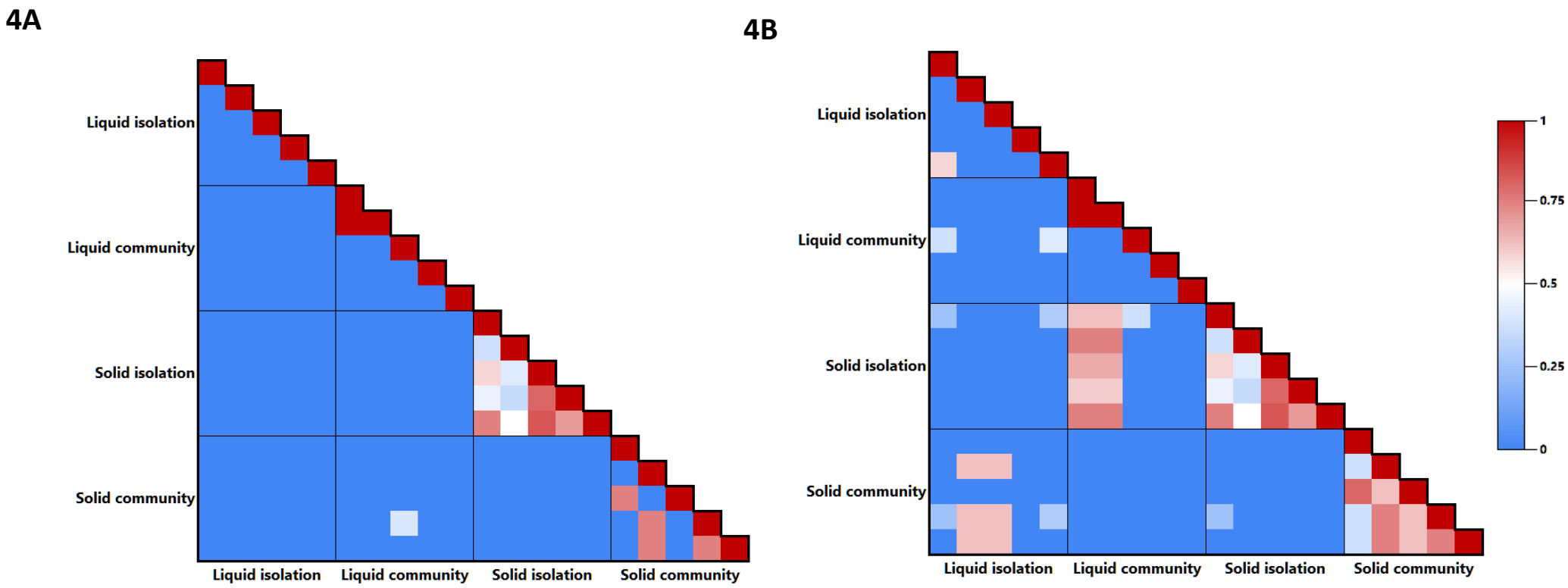

Figure 4 | Clustering and mutation repeatability of final replicates clustered on gene and COG level. The level of genetic parallelism in evolved clones is given by the *H*-index. Higher *H*-index values indicate a higher parallelism of the two genotypes compared. Three clones per replicate were sequenced per environment. Comparisons in the blocks around the diagonal in each figure show the intra-environment comparisons, while the other blocks show the inter-environment comparisons. Solid indicates the spatially structured environment and liquid indicates the well-mixed environment. Mutations and genes are shown in Supplementary table 1. **A,** *H*-index of mutation repeatability at the gene-level of *E. coli* mutants. Very few replicates within the well-mixed liquid environment showed repeated evolution, while within the spatially structured environment there was some repeated evolution. **B,** *H*-index of mutation repeatability at the COG-level. Most genetic parallelism is found in the spatially-structured environment, opposing the anticipated higher level of drift in the spatially structured versus well-mixed environments.
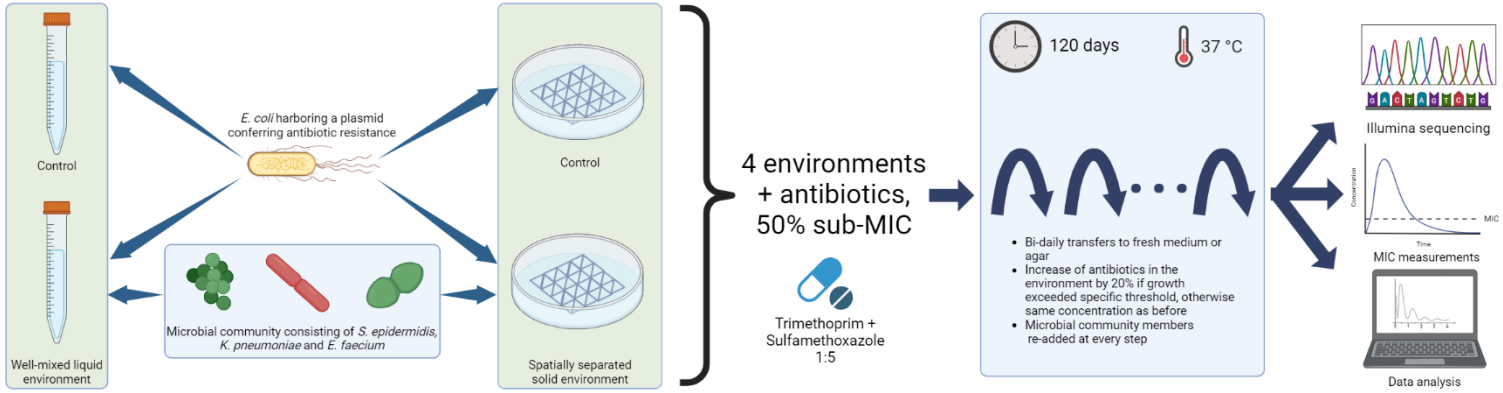
Graphical abstract